

A simple and green approach for the synthesis of substituted dihydro-2-oxypyrrroles catalyzed by nano-Fe₃O₄@SiO₂/SnCl₄ superparamagnetic nanoparticles

Bi Bi Fatemeh Mirjalili^{a,*}, Reza Araqi^a, Seyed Ahmad Mohajeri^b

^aDepartment of Chemistry, College of Science, Yazd University, Yazd, P.O. Box. 89195-741, I. R. Iran.

^bPharmaceutical Research Center, School of pharmacy, Mashhad University of Medical Sciences, Mashhad, Iran.

Received 5 August 2017; received in revised form 2 March 2018; accepted 6 March 2018

ABSTRACT

In this work, an efficient and green procedure for the synthesis of dihydro-2-oxypyrrroles has been developed. One-pot four-component condensation reaction of aniline derivatives (2 mmol), dialkyl acetylene dicarboxylate (1 mmol), and aldehydes (1 mmol) was done in ethanol at 65 °C in the presence of nano-Fe₃O₄@SiO₂/SnCl₄ as a magnetically reusable heterogeneous acid catalyst. The obtained dihydro-2-oxypyrrroles were purified without any chromatography techniques. The structure of obtained pure products was identified by physical properties and spectroscopic data such as FT-IR, ¹H NMR, ¹³C NMR and mass spectroscopy. This protocol consistently has the advantages of excellent yields, short reaction time, simple workup, recyclability of the catalyst up to six runs without appreciable loss of activity.

Keywords: Dihydro-2-oxypyrrroles, Nano-Fe₃O₄@SiO₂/SnCl₄, Heterogeneous acid catalyst, Magnetic catalyst, Dialkyl acetylene dicarboxylate.

1. Introduction

Nitrogen containing heterocyclics plays key roles in pharmaceutical industry and exhibits a wide range of biological activities. Amongst them, five-membered nitrogen heterocyclic compounds such as dihydropyrrol-2-ones (dihydro-2-oxopyrroles) and their analogues are very interesting compounds due to their biological and pharmaceutical activity such as inhibitors of the human immunodeficiency virus (HIV) integrase [1], human mitotic kinesin Eg5 [2], vascular endothelial growth factor receptors (VEGFR) [3], annexin A2-S100A10 protein interaction [4], CD45 protein tyrosine phosphatase [5], anti-influenza [6], antibiotics [7], nootropic agents [8] and herbicidal [9]. In addition, their anti-tumor activity [10] and also useful intermediates [11] increasingly necessitate new research. Structures of some biologically important dihydropyrrol-2-one are shown in Fig. 1.

In synthetic organic chemistry, multicomponent reactions (MCRs) have gained considerable popularity in recent years due to their flexible, convergent, and atom-efficient nature. The MCRs are an ideal synthetic tool to generate multiple molecular scaffolds and to increase structural and skeletal diversity. These reactions which consist of two or more synthetic steps, are carried out without the separation of any intermediates; this reduces time, energy and chemicals consumption [12].

Recently, four-component one-pot condensation of dialkylacetylene dicarboxylate, amines, and

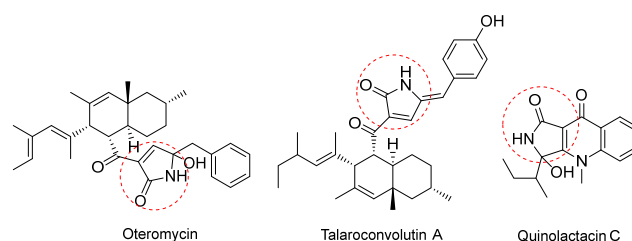


Fig. 1. The structure of some biologically important dihydropyrrol-2-one.

*Corresponding author.

Email address: fmirjalili@yazd.ac.ir (B.B.F. Mirjalili)

formaldehyde has been reported for the construction of substituted dihydro-2-oxypyrrroles using catalytic systems such as Nano-TiCl₄/SiO₂ [13], I₂ [14], Cu(OAc)₂.H₂O [15], BF₃/nano-sawdust [16], TiO₂ nanopowder [17], oxalic acid dehydrate [18], Fe₃O₄@nano-cellulose-OPO₃H [19], nano-Fe₃O₄ [20], trityl chloride (Ph₃CCl) [21], Cu²⁺ [22], 1-methyl-2-oxopyrrolidinium hydrogen sulfate ([Hpyro][HSO₄]) [23], InCl₃ [24], acetic acid [25], [n-Bu₄N][HSO₄] [26], sucrose [27], Al(H₂PO₄)₃ [28] and CoFe₂O₄@SiO₂@IRMOF-3 [29].

Although most of these methods offer distinct advantages, some of them still have their own limitations in terms of yields, longer reaction times and difficult work-up. In some cases, the used catalysts are harmful to environment and cannot be reused. Therefore, an efficient method for the synthesis of substituted dihydro-2 oxypyrrroles is still desirable. In continuation of previous works [19, 30-32], we wish to report an efficient and eco-friendly procedure for the preparation of substituted dihydro-2-oxypyrrroles in the presence of nano-Fe₃O₄@SiO₂/SnCl₄ [33,34].

2. Experimental

2.1. Materials and apparatus

All high purity chemicals and solvents were purchased from the Merck and Fluka Chemical Companies. Materials were of the commercial reagent grade. FT-IR spectra were recorded as the KBr pellet on a Bruker, Equinox 55 spectrometer Perkin-Elmer 781 spectrophotometer. ¹HNMR and ¹³CNMR spectra were recorded at 400 MHz and 100 MHz, respectively, on a Bruker DXR-400 spectrometer. Mass spectra (MS) were recorded on a FINNIGAN-MAT 8430 mass spectrometer, operating at an ionization potential of 70 eV. Melting points were determined by a Buchi melting point B-540 B.V.CHI apparatus. Powder X-ray diffraction (XRD) pattern was obtained by a Philips Xpert MPD diffractometer equipped with a Cu K_α anode (k = 1.54 Å) in the 2θ range from 10 to 80°. Field Emission Scanning Electron Microscopy (FESEM) and Transmission Electron Microscopy (TEM) images of catalyst were obtained on a Mira 3-XMU and Philips CM120 with a LaB₆ cathode and accelerating voltage of 120 kV, respectively. VSM measurements were performed using a vibrating sample magnetometer (Meghnatis Daghigh Kavir Co. Kashan Kavir, Iran). Brunauer-Emmett-Teller (BET) surface area analysis of catalyst was done with the Micromeritics, Tristar II 3020 analyzer. The thermal gravimetric analysis (TGA) was performed under Ar atmosphere using "STA 504" instrument.

2.2. Preparation of nano-Fe₃O₄@SiO₂/SnCl₄

Fe₃O₄@SiO₂ (0.65 g) was dispersed in CHCl₃ (10mL) using the ultrasonic method for 30 min. Subsequently, SnCl₄ (0.16 mL) was added drop wise to dispersed solution of Fe₃O₄@SiO₂ at room temperature under vigorous stirring over a period of 30 min. The resulting suspension was separated using an external magnet, washed with chloroform (20mL), and dried at room temperature to obtain the brown solid product, nano Fe₃O₄@SiO₂/SnCl₄.

2.3. General procedure for the synthesis of dihydro-2-oxypyrrroles

All of reactions were run with the following steps: (a) dialkyl acetylenedicarboxylate **1** (1 mmol) and primary amines **2** (1 mmol) were added into round bottomed flask with 5 mL of EtOH, the mixture was stirred for 10-15 min at room temperature; (b) primary amines **3** (1 mmol), aldehydes **4** (1 mmol) or formaldehyde 37% in methanol **4** (1.5 mmol), and nano-Fe₃O₄@SiO₂/SnCl₄ (0.04 g) were added into a test tube containing 2 mL of H₂O, then the mixture in the test tube was added into the above mixture in the round bottomed flask, and stirred at 65 °C for the appropriate time (Table 2). Upon completion of the reaction, as indicated by TLC, the catalyst was easily removed by an external magnet and reused in subsequent reactions. After removing the catalyst, the mixture was allowed to cool, filtered off and washed with EtOH (3 × 2 ml) and recrystallized from ethanol to afford the pure products **5**.

3. Results and Discussion

To study of the structure of catalyst, the FT-IR spectra of nano-Fe₃O₄, nano-Fe₃O₄@SiO₂, and nano-Fe₃O₄@SiO₂/SnCl₄ were compared (Fig. 2). Nano-Fe₃O₄ was identified by bands at 443 and 560 cm⁻¹ due to Fe/O vibrations (Fig. 2a). The FT-IR spectrum of nano-Fe₃O₄@SiO₂ displays characteristic peaks at 1094 and 802 cm⁻¹ for Si-O-Si vibration. Weak band at 469 cm⁻¹ corresponds to the Si-O/Fe vibrations of the nano-Fe₃O₄@SiO₂. The successful covalent linking of the SnCl₄ on the surface of nano-Fe₃O₄@SiO₂ was confirmed by the appearance of new bands in 1405 and 426 cm⁻¹, that originates from the absorption of Si-O-Sn (Fig. 2d).

XRD patterns of nano-Fe₃O₄, nano-Fe₃O₄@SiO₂, and nano-Fe₃O₄@SiO₂/SnCl₄ were shown in Fig. 3. Nano-Fe₃O₄@SiO₂ exhibited a broadened pattern due to the non-crystalline nature at 2θ= 20-30 corresponding to amorphous phase of SiO₂. Also, the catalyst showed peaks at 30.33, 35.79, 43.36, 53.82, 57.36, 62.99 and 74.62°, which corresponded to nano-Fe₃O₄ structures.

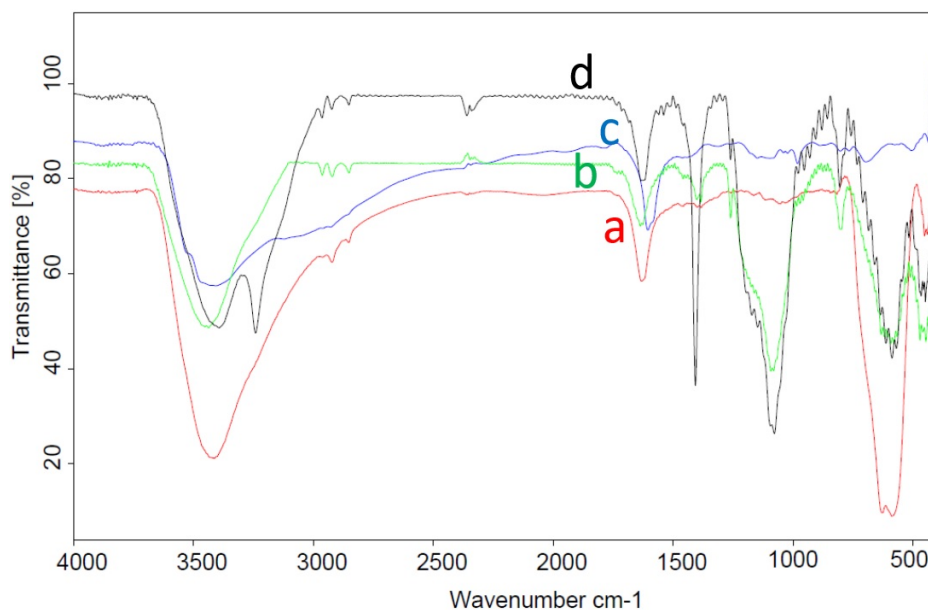


Fig. 2. FT-IR spectra of (a) nano-Fe₃O₄, (b) nano-Fe₃O₄@SiO₂, (c) SnCl₄ and (d) nano-Fe₃O₄@SiO₂/SnCl₄.

The additional peaks such as 10, 34 and 50° in XRD pattern of nano-Fe₃O₄@SiO₂/SnCl₄ can indicate SnCl₄ presence in the catalyst structure.

The energy dispersive X-ray (EDX) from the nano-Fe₃O₄@SiO₂/SnCl₄ (Fig. 4) indicated the presence of the expected elements in the structure of this catalyst and confirmed supporting of SnCl₄ on nano-Fe₃O₄@SiO₂. The elemental compositions of nano-Fe₃O₄@SiO₂/SnCl₄ were found to be 52.80, 31.33,

0.82, 5.30 and 9.76% for Fe, O, Si, Sn and Cl, respectively.

To investigate the magnetic property of catalyst, magnetic measurements were carried out using a vibrating sample magnetometer (VSM) in an applied magnetic field at 300 K (Fig. 5). As shown in VSM patterns, not only were hysteresis loop and remanence detected but also the coercivity value is zero for all samples.

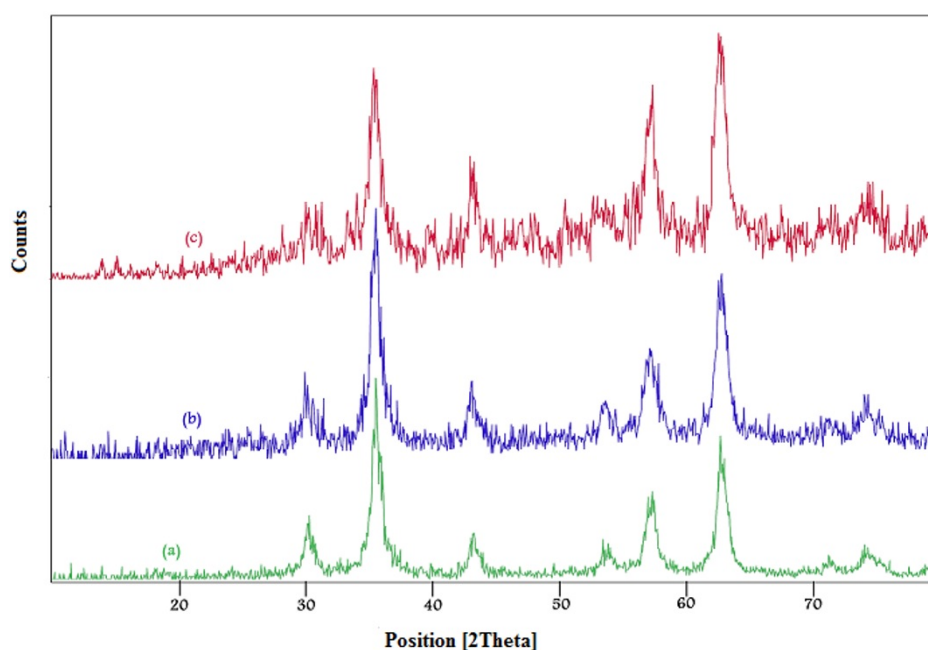


Fig. 3. XRD patterns of (a) nano-Fe₃O₄, (b) nano-Fe₃O₄@SiO₂, and (c) nano-Fe₃O₄@SiO₂/SnCl₄.

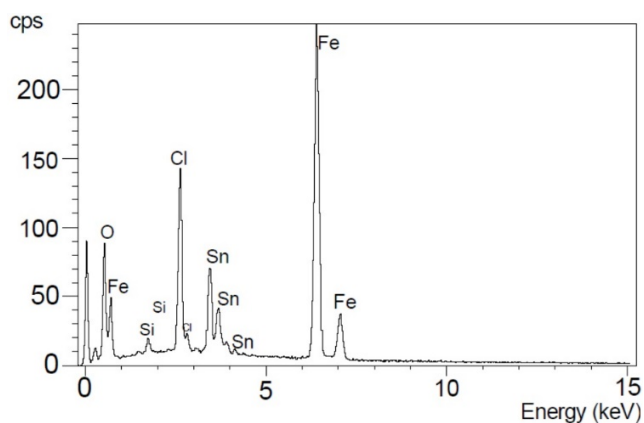


Fig. 4. EDX patterns of nano-Fe₃O₄@SiO₂/SnCl₄.

This VSM pattern suggests a typical superparamagnetic property for catalyst at room temperature. The saturation magnetization (*M_s*) values of nano-Fe₃O₄, nano-Fe₃O₄@SiO₂ and nano-Fe₃O₄@SiO₂/SnCl₄ are 53.52, 40.98 and 31.05 emu g⁻¹, respectively. These results indicate that the magnetization of nano-Fe₃O₄ was considerably decreased by coating it with SiO₂ and bonding SnCl₄ to OH groups of SiO₂.

The FESEM images of the nano-Fe₃O₄, nano-Fe₃O₄@SiO₂, and nano-Fe₃O₄@SiO₂/SnCl₄ nanoparticles are displayed in Fig. 6. These images evidently show the surface morphology of three kinds of synthesized MNPs with a nearly spherical shape. Nano-Fe₃O₄@SiO₂ and nano-Fe₃O₄@SiO₂/SnCl₄ keep the morphology of nano-Fe₃O₄ with slightly larger particle size.

Transmission electron microscopy (TEM) image of the synthesized catalyst was recorded as depicted in Fig. 7. According to this image, the catalyst size was approximately 28 nm.

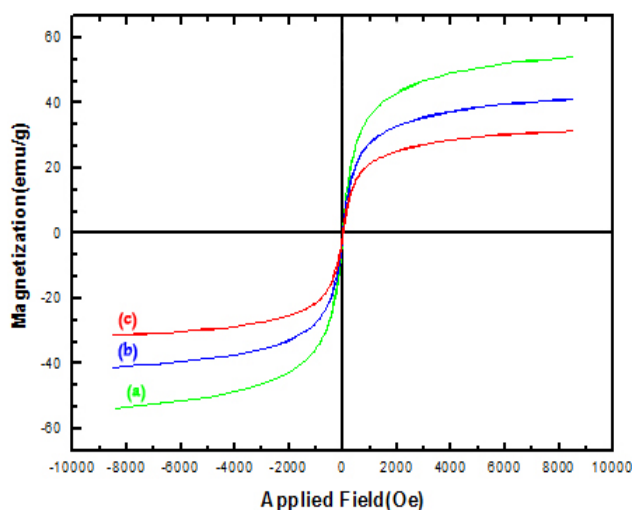


Fig. 5. VSM patterns of (a) nano-Fe₃O₄, (b) nano-Fe₃O₄@SiO₂ and (c) nano-Fe₃O₄@SiO₂/SnCl₄.

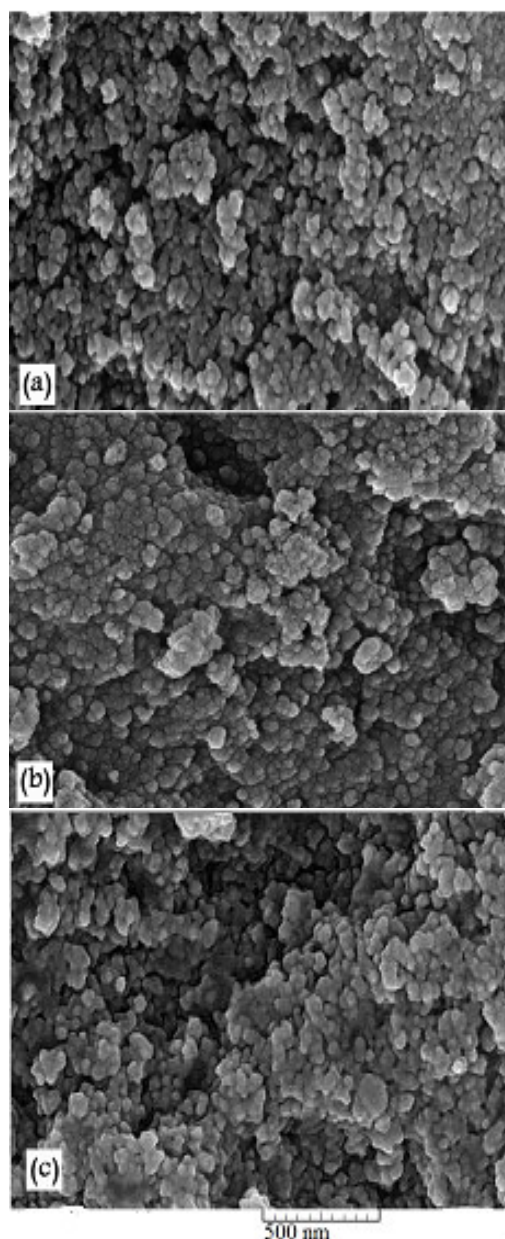


Fig. 6. FESEM images of (a) nano-Fe₃O₄, (b) nano-Fe₃O₄@SiO₂, and (c) nano-Fe₃O₄@SiO₂/SnCl₄.

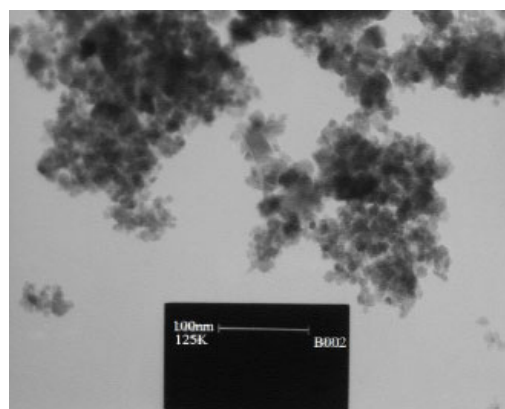


Fig. 7. TEM image of nano-Fe₃O₄@SiO₂/SnCl₄.

The thermal gravimetric analysis (TG-DTA) pattern of nano-Fe₃O₄@SiO₂/SnCl₄ NPs was also performed when heat increased from 100 °C to 750 °C, showing the percent of weight losses (Fig. 8). According to the curves, the 10 % and 15 % weight loss in the temperature 200-250 °C and 300–750 °C ranges can be attributed to the water desorption (exothermic). The char yield in 750 °C is 30 %. These observations show that the catalyst is stable up to 200 °C.

Brunauer–Emmett–Teller (BET) theory was applied to measure the specific surface area of catalyst. The single point surface area was 59.0467 m² g⁻¹ at $P/P_0 = 0.111$. The N₂ adsorption isotherm of catalyst was shown in Fig. 9.

To develop efficient and environmentally friendly protocols for the synthesis of biologically important heterocyclic products, substituted dihydro-2-oxypyrrole derivatives were synthesized *via* one-pot four-component domino reaction of aniline derivatives, dialkyl acetylenedicarboxylates, and an aldehyde in the presence of a nano-Fe₃O₄@SiO₂/SnCl₄ in ethanol under reflux conditions.

The structure of obtained products were characterized by FT-IR, ¹H, and ¹³CNMR spectroscopy. In order to initially evaluate the catalytic reactivity of nano-Fe₃O₄@SiO₂/SnCl₄, the synthesis of methyl-1-(4-chlorophenyl)-4-((4-chlorophenyl)amino)-5-oxo-2,5-dihydro-1*H*-pyrrole-3-carboxylate (**5a**) in various conditions was examined (Scheme 1, Table 1).

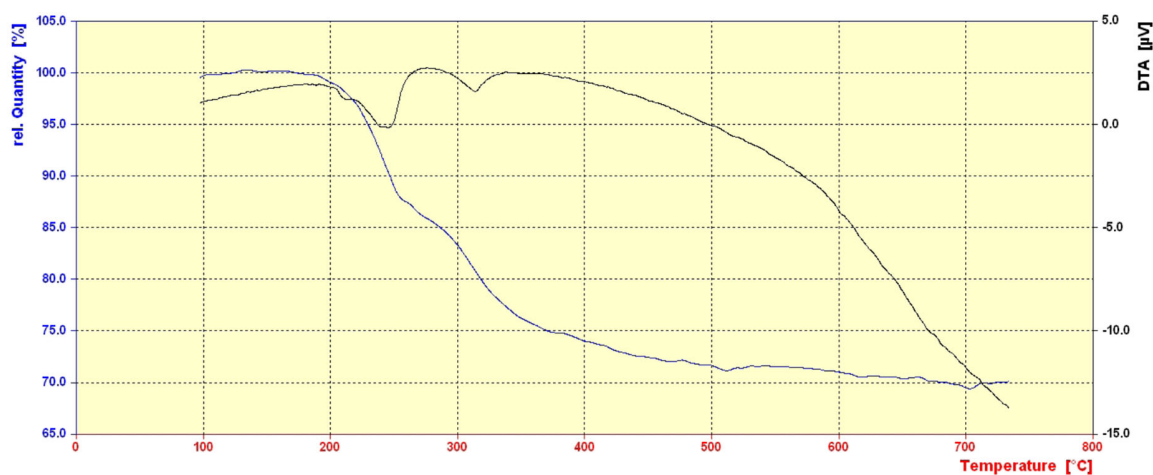


Fig. 8. TGA/DTA pattern of nano-Fe₃O₄@SiO₂/SnCl₄.

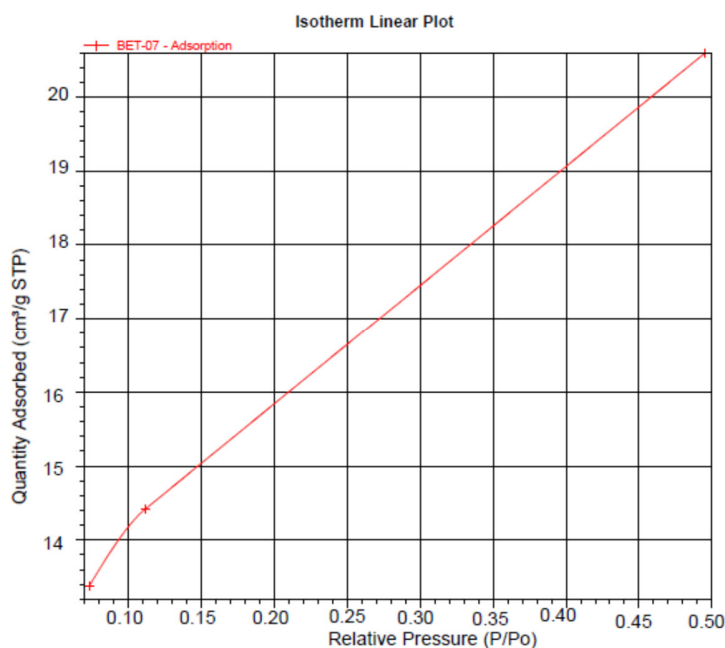
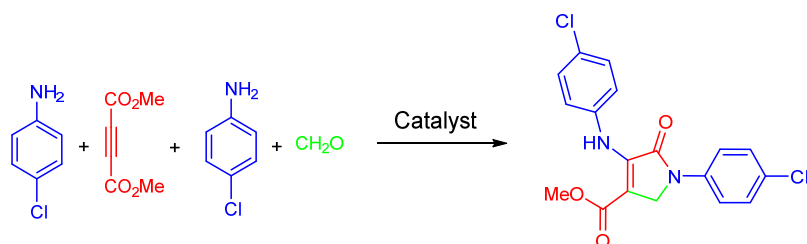


Fig. 9. Adsorption/desorption isotherm pattern of nano-Fe₃O₄@SiO₂/SnCl₄.



Scheme 1. Synthesis of methyl-1-(4-chlorophenyl)-4-((4-chlorophenyl)amino)-5-oxo-2,5-dihydro-1H-pyrrole-3-carboxylate as a model reaction

Table 1. The optimization of condition for condensation of 4-chloroaniline (2 mmol) with dimethyl acetylenedicarboxylate (1 mmol) and formaldehyde (1.5 mmol).

Entry	Catalyst (g)	Solvent/Temp. (°C)/Time (h)	Yield (%) ^a	Ref.
1	-	EtOH/ r. t./20	Trace	-
2	Nano-Fe ₃ O ₄ (0.02)	EtOH/ r. t./7	60	-
3	SiO ₂ /SnCl ₄ (0.02)	EtOH/ r. t./6	65	-
4	SnCl ₄ (0.02)	EtOH/ r. t./10	40	-
5	Nano-Fe ₃ O ₄ @SiO ₂ /SnCl ₄ (0.02)	EtOH/ r. t./6	50	-
6	Nano-Fe ₃ O ₄ @SiO ₂ /SnCl ₄ (0.02)	MeOH/ r. t./7	45	-
7	Nano-Fe ₃ O ₄ @SiO ₂ /SnCl ₄ (0.02)	Acetone/ r. t./9	30	-
8	Nano-Fe ₃ O ₄ @SiO ₂ /SnCl ₄ (0.02)	CH ₃ CN/ r. t./15	Trace	-
9	Nano-Fe ₃ O ₄ @SiO ₂ /SnCl ₄ (0.02)	H ₂ O/ r. t./10	20	-
10	Nano-Fe ₃ O ₄ @SiO ₂ /SnCl ₄ (0.02)	HOAc/ r. t./20	Trace	-
11	Nano-Fe ₃ O ₄ @SiO ₂ /SnCl ₄ (0.02)	-/80/10	Trace	-
12	Nano-Fe ₃ O ₄ @SiO ₂ /SnCl ₄ (0.02)	EtOH/35/8	55	-
13	Nano-Fe ₃ O ₄ @SiO ₂ /SnCl ₄ (0.02)	EtOH/45/6	60	-
14	Nano-Fe ₃ O ₄ @SiO ₂ /SnCl ₄ (0.02)	EtOH/55/5	65	-
15	Nano-Fe ₃ O ₄ @SiO ₂ /SnCl ₄ (0.02)	EtOH/65/3	70	-
16	Nano-Fe ₃ O ₄ @SiO ₂ /SnCl ₄ (0.02)	EtOH/75/3	65	-
17	Nano-Fe ₃ O ₄ @SiO ₂ /SnCl ₄ (0.03)	EtOH/65/2	80	-
18	Nano-Fe ₃ O ₄ @SiO ₂ /SnCl ₄ (0.04)	EtOH/65/1	97	This work
19	Nano-Fe ₃ O ₄ @SiO ₂ /SnCl ₄ (0.05)	EtOH/65/1	95	-
20	Al(H ₂ PO ₄) ₃ (0.1)	MeOH/ r. t./ 6	81	[28]
21	InCl ₃ (20 mol %)	MeOH/ r. t./ 3	79	[24]
22	Ph ₃ CCl (10 mol %)	EtOH/ r. t./ 4	83	[21]
23	I ₂ (10 mol %)	MeOH/ r. t./ 1	81	[14]
24	Fe ₃ O ₄ @NCs-PA (0.07)	EtOH/ r. t./ 3.5	88	[19]
25	BF ₃ /nano-sawdust (0.08)	EtOH/ Ref./ 3.5	92	[16]
26	Nano-TiCl ₄ /SiO ₂ (0.08)	EtOH/ 70 °C/ 2	95	[13]
27	Cu(OAc) ₂ .H ₂ O (15 mol %)	MeOH/ r. t./ 1	81	[15]
28	[n-Bu ₄ N][HSO ₄] (10 mol%)	MeOH/ r. t./ 4	86	[26]

^aIsolated yield.

For this purpose, one-pot four-component condensation reaction of dimethylacetylene dicarboxylate (1 mmol), 4-chloroaniline (2 mmol) and formaldehyde (1.5 mmol) was done using SnCl_4 , nano- Fe_3O_4 , $\text{SiO}_2/\text{SnCl}_4$ or nano- $\text{Fe}_3\text{O}_4@/\text{SiO}_2/\text{SnCl}_4$ as catalysts. Nano- $\text{Fe}_3\text{O}_4@/\text{SiO}_2/\text{SnCl}_4$ acted as a highly efficient magnetic nano-catalyst to synthesize of **5a** and afforded the product in higher yield and lower reaction time, compared with other catalysts (Table 1). Also, other advantages of the current catalyst are simple separation and recovery of it compared with other reported catalysts. Considering above results, the importance of nano- $\text{Fe}_3\text{O}_4@/\text{SiO}_2/\text{SnCl}_4$ composite as a heterogeneous catalyst was revealed in this study and therefore it was selected as the efficient catalyst for further work.

The efficiency of the supported catalyst was found to be affected by the nature of the solvent and the quantity of the catalyst used in the reaction. In preliminary experiment, this reaction was carried out in various solvents with nano- $\text{Fe}_3\text{O}_4@/\text{SiO}_2/\text{SnCl}_4$ (0.02 g) as a catalyst at ambient temperature. After solvent screening, ethanol was the best choice for this condensation

reaction. The reaction proceeded perfectly in low temperature, but the yields increased when the reaction was carried out in high temperature. The yield of product **5a** was improved and the reaction time was shortened as the temperature increased from room temperature to 65 °C, no further improvement was observed at 75 °C (Table 1, Entries 8-12). Therefore, the most suitable reaction temperature is 65 °C.

The reaction slowly proceeded in low yield without catalyst. The higher yield of the corresponding product was obtained in the shorter time with an increase in the amount of magnetic nanocatalyst. As can be seen from Table 1, comparison of the results shows a better yield (97%) using 0.04 g of catalyst nano- $\text{Fe}_3\text{O}_4@/\text{SiO}_2/\text{SnCl}_4$ to synthesize of (**5a**). While a higher amount of the catalyst did not show any change in the reaction time and yield of the corresponding product. Utilizing the optimum reaction conditions, the substrate scope of this reaction was investigated using a variety of aldehydes, amines and dimethyl and/or diethyl acetylenedicarboxylates and the results are summarized in Table 2.

Table 2. Synthesis of dihydro-2-oxopyrrole derivatives in the presence of nano- $\text{Fe}_3\text{O}_4@/\text{SiO}_2/\text{SnCl}_4$ at 65 °C.

Entry	R ¹	R ²	R ³	R ⁴	Prod.	Time (min)	Yield (%) ^a	m.p. (°C)		Ref.
								Found	Reported	
1	4-Cl-C ₆ H ₄	Me	4-Cl	H	5a	60	97	173–174	175–176	[16]
2	4-Cl-C ₆ H ₄	Et	4-Cl	H	5b	65	96	167–168	168–170	[19]
3	4-Br-C ₆ H ₄	Me	4-Br	H	5c	60	96	181–182	181–182	[19]
4	4-Br-C ₆ H ₄	Et	4-Br	H	5d	65	94	165–166	164–165	[16]
5	4-NO ₂ -C ₆ H ₄	Et	4-NO ₂	H	5e	80	87	204–206	207–208	[19]
6	3-NO ₂ -C ₆ H ₄	Me	3-NO ₂	H	5f	70	89	190–192	190–191	[19]
7	3-NO ₂ -C ₆ H ₄	Et	3-NO ₂	H	5g	70	90	206–208	204–206	[19]
8	4-Me-C ₆ H ₄	Me	4-Me	H	5h	50	94	175–176	175–176	[16]
9	4-Me-C ₆ H ₄	Et	4-Me	H	5i	55	92	128–130	131–132	[19]
10	4-Et-C ₆ H ₄	Me	4-Et	H	5j	50	97	124–126	124–125	[19]
11	4-Et-C ₆ H ₄	Et	4-Et	H	5k	50	94	98–100	102–104	[16]
12	4-OMe-C ₆ H ₄	Me	4-OMe	H	5l	60	90	160–162	102–104	[19]
13	4-OMe-C ₆ H ₄	Et	4-OMe	H	5m	65	89	152–153	153–154	[16]
14	4-Cl-C ₆ H ₄	Me	4-Cl	C ₆ H ₅	5n	80	95	175–177	176–177	[19]
15	4-Cl-C ₆ H ₄	Me	4-Cl	4-Me-C ₆ H ₄	5o	80	96	148–150	150–151	[16]
16	PhCH ₂	Me	4-Br	C ₆ H ₅	5q	75	97	154–156	152–154	[19]
17	PhCH ₂	Et	H	H	5r	80	98	138–140	139–141	[16]

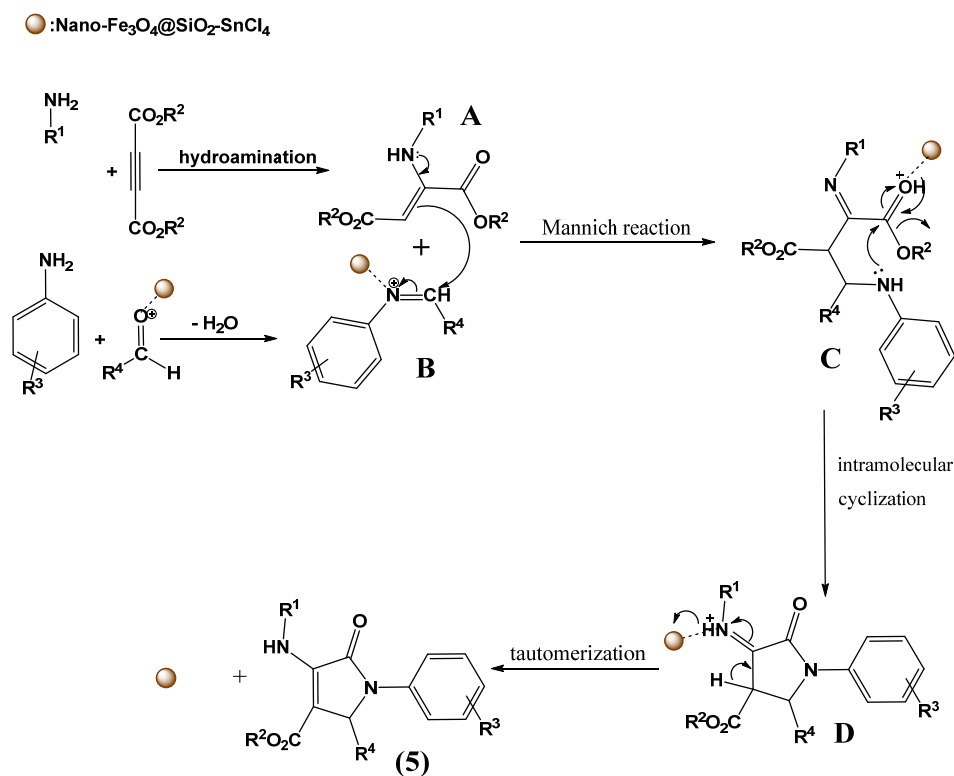
^aIsolated yields.

In general, the reactions proceeded cleanly and the desired *N*-aryl-3-aminodihydropyrrol-2-one-4-carboxylates were obtained in reasonable yields (Table 2, Entries 1–15). Additionally, two different amines were used for the one-pot four-component synthesis of different highly functionalized dihydropyrrol-2-ones. Encouraged by these results, different polyfunctionalized dihydropyrrol-2-ones **5p–r** were synthesized using two different amines. Aliphatic amines, such as benzylamine, were reacted with dialkyl acetylenedicarboxylates, aromatic amines and aldehyde to produce the corresponding products in high yields (Table 2, Entries 16–17). It is interesting to note that the pure products in all reactions can be obtained by simple filtration and recrystallization in ethanol without any tedious isolation and chromatography. The structures of the compounds were characterized by IR, ^1H , and ^{13}C NMR, and mass spectroscopy and elemental analysis and the structures of known products were confirmed by comparison of their melting points and spectral data (IR, ^1H and ^{13}C NMR) with those of authentic samples.

A possible reaction mechanism is suggested in scheme 2. First, the reaction of amine **1** with dialkyl acetylenedicarboxylate **2** leads to intermediate **A** and condensation between amine **3** and aldehyde **4** in the

presence of nano- $\text{Fe}_3\text{O}_4@\text{SiO}_2/\text{SnCl}_4$, which can act as Lewis acid catalyst (empty *p* orbital of Sn in nano- $\text{Fe}_3\text{O}_4@\text{SiO}_2/\text{SnCl}_4$) produces imine **B**. Then, intermediate **A** undergoes Mannich type reaction with imine **B** to furnish reactive intermediate **C**, which is converted to intermediate **D** by cyclization reaction. Finally, intermediate **D** tautomerizes to the corresponding dihydro-2-oxopyrroles **5**.

It is commercially important that solid acids retain their acidic properties even after several uses. Thus, the reusability of nano- $\text{Fe}_3\text{O}_4@\text{SiO}_2-\text{SnCl}_4$ catalyst was also checked. For this aim, the model reaction was examined under optimized conditions. When the reaction was completed, the catalyst was separated from the reaction mixture using an external magnetic field and was washed with hot ethanol. The recycled catalyst was heated in an oven at temperature of 80°C for 1 h and was used for next run. The recycled catalyst could be reused 6 times without significant decreasing in its catalytic activity. The XRD of the recovered magnetic nanocatalyst was shown in Fig. 10. There is no considerable change in its magnetic phase. The leaching of the catalyst should also be examined and leaching was not observed in this protocol. Therefore, the nanocatalyst is stable during synthesis of substituted dihydropyrrol-2-ones under optimized conditions.



Scheme 2. Proposed mechanism for the synthesis of dihydro-2-oxopyrroles in the presence of nano- $\text{Fe}_3\text{O}_4@\text{SiO}_2/\text{SnCl}_4$.

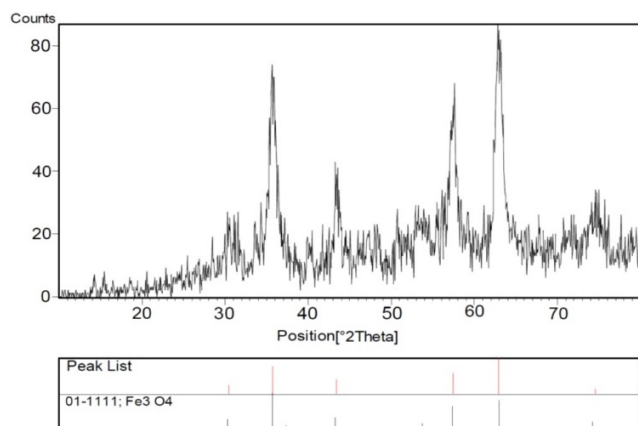


Fig. 10. XRD patterns of recovered nano-Fe₃O₄@SiO₂/SnCl₄ after five recovery.

4. Conclusions

The magnetically recoverable nano-Fe₃O₄@SiO₂/SnCl₄ MNPs are found to be more efficient for the synthesis of highly functionalized dihydro-2-oxopyrroles via one-pot four-component reaction of amines, dialkyl acetylenedicarboxylates and aldehydes in EtOH at 65 °C. The salient features are mild and green reaction conditions, high yields, short reaction times, simple experimental procedure, simplicity in operation, no requirement for chromatography chromatography, and the use of easily recyclable catalyst without loss of considerable catalytic activity. In addition, low cost, availability, recyclability and low toxicity of the catalyst make this method a valid contribution to the existing processes in the field of one-pot multicomponent reaction.

Acknowledgements

The Research Council of Yazd University is gratefully acknowledged for the financial support for this work.

References

- [1] T. Kawasuji, M. Fuji, T. Yoshinaga, A. Sato, T. Fujiwara, R. Kiyama, *Bioorgan. Med. Chem.* 15 (2007) 5487-5492.
- [2] X. Luo, M. Shu, Y. Wang, J. Liu, W. Yang, Z. Lin, *Molecules* 17 (2012) 2015-2029.
- [3] C. Peifer, R. Selig, K. Kinkel, D. Ott, F. Totzke, C. Schächtele, R. Heidenreich, M. Röcken, D. Schollmeyer, S. Laufer, *J. Med. Chem.* 51 (2008) 3814-3824.
- [4] T.R. Reddy, C. Li, X. Guo, H.K. Myrvang, P.M. Fischer, L.V. Dekker, *J. Med. Chem.* 54 (2011) 2080-2094.
- [5] W. R. Li, S.T. Lin, N.M. Hsu, M.S. Chern, *J. Org. Chem.* 67 (2002) 4702-4706.
- [6] A. Kolocouris, G.B. Foscolos, G. Fytas, J. Neyts, E. Padalko, J. Balzarini, R. Snoeck, G. Andrei, E. De Clercq, *J. Med. Chem.* 39 (1996) 3307-3318.
- [7] A.S. Demir, F. Aydogan, I.M. Akhmedov, *Tetrahedron Asym.* 13 (2002) 601-605.
- [8] Z. Feng, X. Li, G. Zheng, L. Huang, *Bioorg. Med. Chem. Lett.* 19 (2009) 2112-2115.
- [9] L. Zhang, Y. Tan, N.X. Wang, Q.Y. Wu, Z. Xi, G.F. Yang, *Bioorg. Med. Chem.* 18 (2010) 7948-7956.
- [10] S. Tarnavsky, G. Dubinina, S. Golovach, S. Yarmoluk, *Biopolym. Cell.* 19 (2003) 548-552.
- [11] D. Albrecht, B. Basler, T. Bach, *J. Org. Chem.* 73 (2008) 2345-2356.
- [12] A. Dömling, *Chem. Rev.* 106 (2006) 17-89.
- [13] A. Bamoniri, B.F. Mirjalili, R. Tarazian, *Monatsh. Chem.* 146 (2015) 2107-2115.
- [14] A.T. Khan, A. Ghosh, M. M. Khan, *Tetrahedron Lett.* 53 (2012) 2622-2626.
- [15] L. Lv, S. Zheng, X. Cai, Z. Chen, Q. Zhu, S. Liu, *ACS Comb. Sci.* 15 (2013) 183-192.
- [16] B.F. Mirjalili, R. Zare Reshquiyea, *RSC Adv.* 5 (2015) 15566-15571.
- [17] S. Rana, M. Brown, A. Dutta, A. Bhaumik, C. Mukhopadhyay, *Tetrahedron Lett.* 54 (2013) 1371-1379.
- [18] S.S. Sajadikhah, N. Hazeri, M.T. Maghsoodlou, S.M. Habibi-Khorassani, K. Khandan-Barani, *J. Chem. Res.* 37 (2013) 40-42.
- [19] N. Salehi, B.F. Mirjalili, *RSC Adv.* 7 (2017) 30303-30309.
- [20] M. Nickraftar, N. Najafi Hajivar, J. Aboonajmi, E. Fereidooni, *Res. Chem. Intermed.* 42 (2016) 2899-2908.
- [21] S.S. Sajadikhah, M.T. Maghsoodlou, *RSC Adv.* 4 (2014) 43454-43459.
- [22] L. Lv, S. Zheng, X. Cai, Z. Chen, Q. Zhu, S. Liu S, *ACS Comb. Sci.* 15 (2013) 183-192;
- [23] S.S. Sajadikhah, N. Hazeri, M.T. Maghsoodlou, S.M. Habibi-Khorassani, *J. Chin. Chem. Soc.* 60 (2013) 1003-1006.
- [24] S.S. Sajadikhah, M.T. Maghsoodlou, N. Hazeri, *Chin. Chem. Lett.* 25 (2014) 58-60.
- [25] Q. Zhu, H. Jiang, J. Li, S. Liu, C. Xia, M. Zhang, (2009) *J. Comb. Chem.* 11 (2009) 685-696.
- [26] S.S. Sajadikhah, N. Hazeri, *Res. Chem. Intermed.* 40 (2014) 737-748.
- [27] N. Hazeri, S.S. Sajadikhah, M.T. Maghsoodlou, S. Mohamadian-Souri, M. Norouzia, M. Moein, *J. Chin. Chem. Soc.* 61 (2014) 217-220.
- [28] S.S. Sajadikhah, N. Hazeri, M.T. Maghsoodlou, S.M. Habibi-Khorassani, A. Beigbabaei, A.C. Willis, *J. Iran. Chem. Soc.* 10 (2013) 863-871.
- [29] J.N. Zhang, X.H. Yang, W.J. Guo, B. Wang, Z.H. Zhang, *Synlett* 28 (2017) 734-740.
- [30] B.F. Mirjalili, H. Jorsarraie, H. Akrami, *Iran. J. Catal.* 7 (2017) 201-205.
- [31] B.F. Mirjalili, A. Bamoniri, Z. Fazeli, *Iran. J. Catal.* 6 (2016) 253-259.
- [32] B.F. Mirjalili, A. Bamoniri, M.A. Mirhoseini, *Iran. J. Catal.* 6 (2016) 23-27.
- [33] B.F. Mirjalili, A. Bamoniri, S. Fouladgar, *Polycycl. Aromat. Compd.* 37 (2017) 345-361.
- [34] A. Bamoniri, S. Fouladgar, *RSC Adv.* 5 (2015) 78483-78490.